Stabilization of Interchange Modes in Mirror Plasmas by a Nonlinear rf-Plasma Wave Coupling Process

Hogun Jhang, S. G. Lee, S. S. Kim, B. H. Park, and J. G. Bak
Korea Basic Science Institute, 52, Yeoeun-dong, Yusung-Gu, Daejon, Korea
(Received 12 November 2004; published 15 July 2005)

Experimental and theoretical studies are made of the consequences of a nonlinear coupling process between pump rf waves and interchange modes in mirror plasmas. It is demonstrated that the interchange-stable operation window exists depending on the applied rf power and $\gamma = \omega_0/\Omega_i$, where ω_0 (Ω_i) is the angular frequency of the applied rf wave (ion cyclotron frequency). Results are shown that the nonlinear wave coupling process gives rise to the operation window near the resonance ($\gamma \simeq 1$), which is elucidated by theoretical analyses combined with full rf wave simulations.

DOI: 10.1103/PhysRevLett.95.035005 PACS numbers: 52.35.Bj, 52.35.Hr, 52.35.Mw, 52.55.Jd

The study of nonlinear interactions between applied rf waves and collective modes of a magnetically confined plasma is a subject of not only theoretical but also practical importance in plasma physics since most magnetic confinement devices employ high power rf waves for the purposes of plasma production and heating. An outstanding example of such a nonlinear interaction is the (de)stabilization of interchange modes in magnetic mirror plasmas by the rf waves in the ranges of ion cyclotron frequency [1–12].

It has been reported that rf waves influence the interchange stability in mirror plasmas by the generation of a radial equilibrium ponderomotive force (EPF) [1–7] and the nonlinear sideband wave coupling (SBC) process [8,9]. The radial amplitude gradient of the rf wave generates the EPF, which is negative or positive depending on the sign of the gradient and the ratio $\gamma = \omega_0/\Omega_i$, where ω_0 is the angular frequency of the rf wave and Ω_i is the ion cyclotron frequency. If the direction of the EPF is radially outward, the EPF causes destabilizing influences on the interchange modes while the opposite gives rise to stabilizing effects on them. The physical mechanism of the SBC is analogous to the nonlinear parametric process [13]. The nonlinear coupling between the interchange mode and the pump rf wave generates sideband waves with wave vectors $\mathbf{k}_\pm = \mathbf{k}_0 \pm \mathbf{k}$ and frequencies $\omega_\pm = \omega_0 \pm \omega$. Here, $\mathbf{k}$ and ω denote the wave vector and the frequency of the interchange mode involved, respectively, and $\mathbf{k}_0$ is the wave vector of the rf wave. Then, the nonlinear beating of the rf wave with the sideband waves produces a low frequency ponderomotive force, affecting the interchange stability [9]. Since both effects will be concomitant in a single plasma discharge, it is of importance to keep both for the interpretation of experimental results [10–12].

Most of the previous experimental [1–5] and theoretical [6,7] studies have attributed the observed enhancement of the stability to the rf-generated EPF. The efficacy of the SBC process on the interchange stability has been regarded to be weak or negligible [12]. In this Letter, we report the first experimental observations of the stability enhancement due to the nonlinear rf-interchange mode interaction in the HANBIT mirror device [14]. A theory combined with full rf wave simulations successfully reproduces the feature of HANBIT experiments, as will be shown shortly.

The HANBIT device is a magnetic mirror machine, consisting of a central cell, an anchor cell, a plug cell, a fan-out tank, and a cusp tank [14]. The axial length and the plasma radius of the central cell are 420 and 16 cm, respectively. The rf antenna is located at $(r, z) = (20.0, 45.0)$ in the central cell, where r and z represent the radial and axial positions in cm units, respectively. The current path and the resulting rf-plasma coupling of the antenna are similar to those of Nagoya Type-III antenna [15]. The rf frequency is normally fixed at 3.5 MHz. The neutral pressure in the central cell is $\sim 1.0 \times 10^{-2}$ mtorr, making the effects of ion-neutral collisions on interchange modes non-negligible ($\nu_{\text{in}} \sim 10$ kHz). Two gas boxes that are located at $z = \pm 100$ provide the hydrogen fuel gas puffing for the plasma production.

In normal HANBIT discharges, we have observed the operation window within which a plasma discharge is carried out successfully, in a reproducible manner. A successful plasma discharge is obtained with a good line density behavior when discharge conditions are within the operation window, whereas the discharge is brought to an end by either plasma production failure or discharge termination when the conditions are outside of it. The operation window has been found to be sensitive to the applied rf power and the value $\gamma = \omega_0/\Omega_i$ with a preference to $\gamma \lesssim 1$. An increase of rf power generally results in an expansion of the operation window into the $\gamma > 1$ region while the decrease of it brings about the reduction of the operation window. It had been conjectured that the existence of the operation window was due to the rf contribution to the interchange stability. In the experiments reported here, we operated the device in a simple mirror geometry. Then, it is expected that the interchange stability is governed solely by rf characteristics and the confining magnetic fields.

Probe systems in the device were utilized as main diagnostic tools in the experiments. Two fixed edge probe arrays along the axial direction are used to measure the azimuthal and parallel characteristics of density fluctuations with a 800 KHz sampling rate. The first array (array I) is located at $(r, z) = (8.0, 204.8)$, and the other one (array IV) is placed at $(r, z) = (16.0, -99.9)$. Each array consists of eight single probe tips (every $\pi/4$ in the azimuthal direction). The radial electron temperature and density profiles of the central cell plasma are measured by a movable triple Langmuir probe, which is placed at the midplane. The profile measurements were carried out on a shot by shot basis. Thus, a careful aftershot analysis has been performed to ensure the identity of each experiment. A magnetic probe array, which is located at $(r, z) = (17.8, 80.2)$, consists of four pickup coils. It measures the azimuthal characteristics of fluctuating magnetic fields with a 10 MHz sampling rate.

Power excursion and modulation experiments were employed for the present study. Figure 1(a) shows the time traces of P_{rf} and line averaged densities for three γ values ($\gamma = 0.99, 1.01, 1.03$) during the power excursion experiments. The rf power is increased to 200 kW for 20 msec, remained flattop for 80 msec, and ramped down to zero with the power variation rate $dP_{\mathrm{rf}}/dt = -1$ kW/msec. During the power excursion period, the plasma passes through the operation window, leading to the discharge termination when P_{rf} is below a threshold value, as shown in Fig. 1(a). When γ is slightly larger than 1, the threshold power increases, resulting in the earlier discharge termination. Hence, the plasma is more vulnerable to the discharge termination when $\gamma \gtrsim 1$, which confirms the empirical observations in normal discharges. Note that a slight change of γ leads to the marked variation of the discharge termination time indicating the sensitivity of the operation window to P_{rf} and γ. The density profile changed little and showed a relatively peaked shape during the power excursion period. Fast Fourier transforms of edge probe data were carried out at different time intervals in order to find the onset time of the plasma termination procedure and the corresponding threshold rf power. The results of the analysis when $\gamma = 1.01$ are shown in Fig. 1(b). A strong and coherent fluctuation centered at $\sim$3 kHz begins to develop from $t = 133$ msec ($P_{\mathrm{rf}} =$ 167 kW). The plasma density begins to collapse $\sim$70 msec after the onset of the edge fluctuation. The fluctuation duration preceding the plasma termination shortens as γ increases.

Figure 2(a) shows the density fluctuations measured by two probes at the same field line along the axial direction. The measured value of $k_{\parallel}$ for the fluctuation is almost zero, indicating that it is a flute mode. The mode rotates with $\sim$3 kHz in the ion diamagnetic direction ($m = -1$), as shown in Fig. 2(b) where the edge plasma densities measured by four probes in array IV are plotted. Thus, the mode

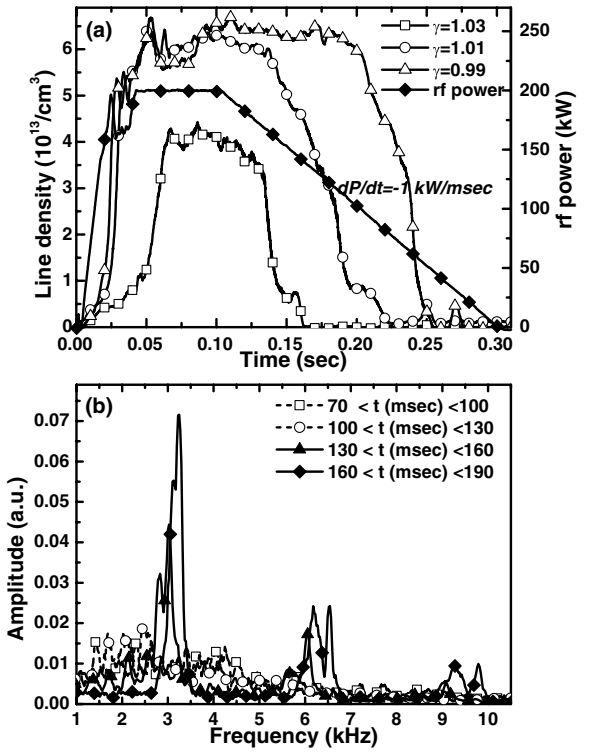

FIG. 1. (a) Evolution of applied rf power and line averaged plasma densities for three values of $\gamma = \omega_0/\Omega_i$ ($\gamma = 1.03, 1.01,$ and 0.99) in power excursion experiments. A slight change of γ leads to a marked variation of the discharge termination time. (b) Fast Fourier transform of an edge probe data in different time intervals ($\gamma = 1.01$). A strong and coherent mode activity centered at $\sim$3 kHz manifests itself from $t \sim 133$ msec.

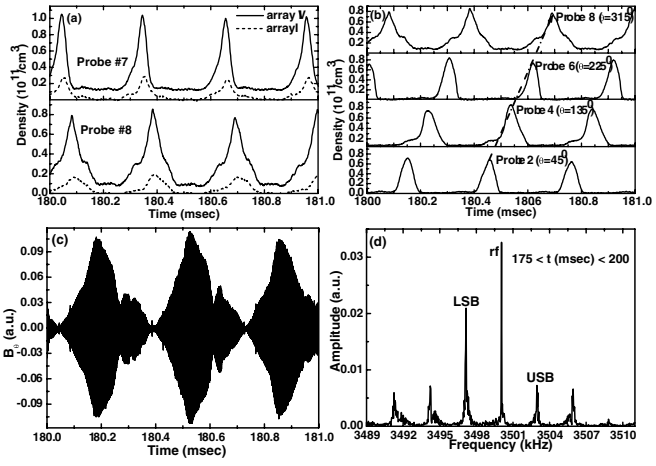

FIG. 2. Edge density fluctuations measured by (a) two probes in the same field line along the axial direction representing a flute mode structure, and (b) four probes in array IV showing $m = -1$ mode structure of the fluctuation. (c) Fluctuating magnetic field measured by a pickup coil showing a strong modulation of the rf wave with the interchange mode. (d) Fast Fourier transform of the magnetic probe data given in (c).

is identified as the $m = -1$ interchange mode. This low frequency $m = -1$ interchange mode was observed for almost all the discharges ending up with a plasma termination, including those given in Fig. 2(a). A similar behavior of the plasma when interchange modes are destabilized has also been reported in the GAMMA 10 tandem mirror when the anchor plasma beta was not sufficient to stabilize the interchange mode in the central cell plasma [16]. A strong modulation of the rf wave with the interchange mode, and the resulting deformation of the wave envelope, was observed as shown in Fig. 2(c), indicating the outset of a strong nonlinear interaction between involved waves. Figure 2(d) represents the fast Fourier transform of the magnetic probe data, showing strong peaks at sideband frequencies $\omega_0 \pm \omega$ as well as at ω_0. The Fourier amplitude of the lower sideband wave is usually stronger than that of the higher one.

The change in density fluctuations when the plasma undergoes stability transition could be seen clearly in power modulation experiments given in Fig. 3(a). As the power increases abruptly at time $t = 130$ msec, the plasma is stabilized and the density fluctuations disappear above a threshold rf power, as can be seen in Fig. 3(b). The threshold rf power is approximately $\sim$170 kW, which agrees well with that of the power excursion experiment.

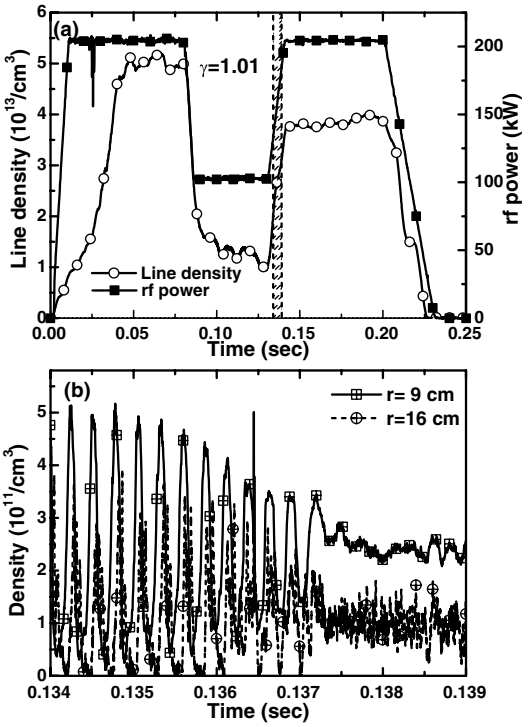

FIG. 3. (a) Evolution of applied rf power and line averaged plasma density in a power modulation experiment ($\gamma = 1.01$). (b) Changes in density fluctuations during the power transition period. The strong fluctuations corresponding to the interchange mode disappear as the rf power increases.

A preliminary analysis of the rf-interchange mode interaction in HANBIT plasmas was carried out in Ref. [17] based on a dissipative two-fluid cold plasma theory combined with Maxwell equations [17]. Following Ref. [17], the dispersion relation for the interchange mode with wave number $\mathbf{k}$ and frequency ω is given by

$$\omega^2 + [(\tau - 1)\omega_{gi} + i\nu_i]\omega + \gamma_G^2 = \gamma_{\mathrm{rf}}^2, \qquad (1)$$

where $\tau = T_e/T_i$, $\omega_{gi} = -kg_i/m_i\Omega_i$ with g_i simulating the centrifugal force originating from field line curvature, ν_i is the ion-neutral collision frequency, $\gamma_G^2 = (k_n/k) \times (\tau + 1)\omega_{gi}\Omega_i$, whose square root yields the growth rate of the interchange mode, and $k_n\hat{r} \equiv \nabla n_0/n_0$. The γ_{rf} in Eq. (1) represents rf effects on the interchange mode. The total rf contribution to the interchange mode is divided into the EPF and the SBC components, $\gamma_{\mathrm{rf}}^2 = \gamma_{\mathrm{SB}}^2 + \gamma_{\mathrm{PM}}^2$, where

$$\gamma_W^2 = \frac{k_n e^2}{m_i^2} \sum_{j=1}^{3} \sum_{\alpha} \frac{\omega_{p\alpha}^2}{\omega_{pi}^2} \times \frac{[(\omega_0 + \sigma_j\Omega_\alpha)K_{1j}^W + i\nu_\alpha K_{2j}^W]}{\omega_0[(\omega_0 + \sigma_j\Omega_\alpha)^2 + \nu_\alpha^2]} |E_{\omega_0}^j|^2 \qquad (2)$$

with $W =$ SB or PM denoting the contribution from the SBC or the EPF, respectively. In Eq. (2), the $\omega_{p\alpha}$ is the plasma frequency of the species α, $\sigma_{(1,2,3)} = (-1, 1, 0)$, and $E_{\omega_0}^j$ is the rf electric field for the jth component. The complication in Eq. (2) comes from the K_j^W terms, the expressions of which are referred to in Ref. [17].

In the preliminary analysis, the experimental feature of the interchange-stable operation window as a function of P_{rf} and γ with a preference to $\gamma \lesssim 1$ was reproduced using a model rf field profile. In order to be more relevant to experiments, however, the rf field profiles should be measured or evaluated using measured plasma parameters. Thus, we combined the theory with a full rf wave simulation code. The exploitation of the full rf wave simulations makes it possible to incorporate the realistic antenna geometry, the axial inhomogeneity of the confining magnetic fields, the effects of nearby conducting structures such as limiters, and the inhomogeneity of density profiles in both axial and radial directions. After confirming that the code satisfies the self-consistent energy conservation law, it was successfully benchmarked with the measured radial rf field profile at an axial position.

The stability analysis is performed by the following procedure. First, we compute radial and axial rf field profiles using measured plasma parameters. Second, the rf fields are decomposed into Fourier components to obtain a $k_{0\|}$ spectrum. The evaluation of k_{0r} is followed by accounting the phase differences between adjacent radial points. We assume that each $\mathbf{k}_0$ component independently contributes to Eq. (2). Finally, we perform the field line and

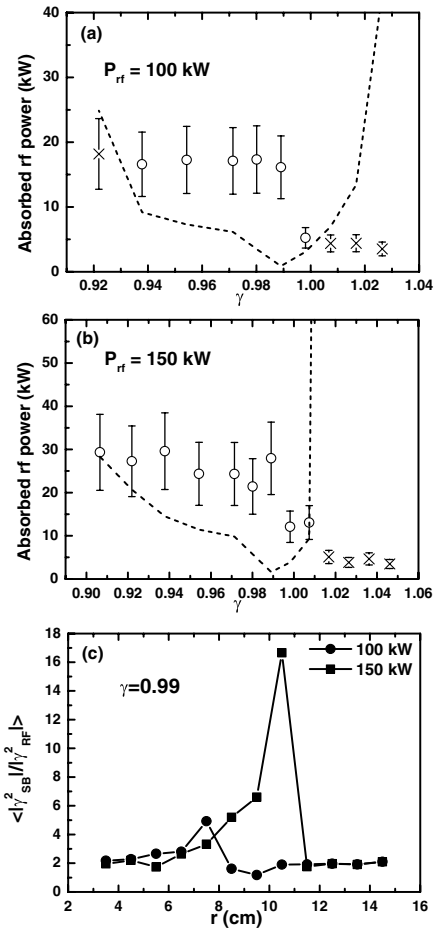

FIG. 4. Comparisons of theoretical predictions and experimental observations when $P_{\rm rf}$ is (a) 100 and (b) 150 kW, respectively. The threshold power was calculated using measured plasma densities and full rf simulations. (c) Field line averaged ratio of SBC to EPF, $\langle|\gamma^2_{\rm SB}|/|\gamma^2_{\rm PM}|\rangle$ as a function of r. Two stable discharges ($\gamma = 0.99$) with $P_{\rm rf} = 100$ (diamond) and 150 (triangle) kW have been used. The SBC is dominant over the EPF for all the ranges of radius.

radial averages of the dispersion relation to evaluate the growth rate of the interchange mode.

Comparisons of theoretical predictions and experimental observations are plotted in Figs. 4(a) and 4(b) when $P_{\rm rf} = 100$ and 150 kW, respectively. In Fig. 4, circles denote stable discharges while "×" marks stand for unstable ones. The uncertainty of the absorbed rf power was accounted for by error bars in Figs. 4(a) and 4(b) from the measurements of reflected rf power. The threshold values of absorbed rf power were calculated by taking measured plasma densities at different γ. As can be seen in Fig. 4, the theory predicts the experimental results with a good precision. The operation window deduced from the theory agrees well with that obtained from HANBIT experiments.

The field line averaged ratio of SBC to EPF, $\langle|\gamma^2_{\rm SB}|/|\gamma^2_{\rm PM}|\rangle$ as a function of radial position is presented in Fig. 4(c). The SBC term is dominant over the EPF term for almost all the ranges of r, indicating that the SBC process is responsible for the observed rf-interchange mode interactions. Hence, the existence of the operation window observed in HANBIT experiments accounts for the stabilization of the interchange mode due to the nonlinear SBC process. The nonlinear SBC process is of significance to the interchange stability near the resonance even in the presence of a strong dissipative process such as neutral collisions.

In conclusion, we observed the interchange-stable operation window in a mirror plasma due to a strong nonlinear wave-wave interaction between the pump rf wave and the interchange mode. Application of a dissipative two-fluid theory combined with full rf simulations revealed the observed feature of the operation window with its sensitivity to the applied rf power and $\gamma = \omega_0/\Omega_i$.

It is a pleasure to acknowledge the technical support of the HANBIT operation team. This work was supported by the Ministry of Korean Science and Technology under the HANBIT project contract.

[1] J. R. Ferron, N. Hershkowitz, R. A. Breun, S. N. Golovato, and R. Goulding, Phys. Rev. Lett. **51**, 1955 (1983).
[2] Y. Yasaka and R. Itatani, Phys. Rev. Lett. **56**, 2811 (1986).
[3] R. Majeski, J. J. Browning, S. Meassick, N. Hershkowitz, T. Intrator, and J. R. Ferron, Phys. Rev. Lett. **59**, 206 (1987).
[4] J. J. Browning, R. Majeski, T. Intrator, N. Hershkowitz, and S. Meassick, Phys. Fluids **31**, 714 (1988).
[5] J. J. Browning, N. Hershkowitz, T. Intrator, R. Majeski, and S. Meassick, Phys. Fluids B **1**, 1692 (1989).
[6] J. R. Myra and D. A. D'Ippolito, Phys. Rev. Lett. **53**, 914 (1984).
[7] D. A. D'Ippolito and J. R. Myra, Phys. Fluids **28**, 1895 (1985).
[8] J. B. McBride, Phys. Fluids **27**, 324 (1984).
[9] J. B. McBride, V. Stefan, and N. A. Krall, Phys. Rev. Lett. **54**, 42 (1985).
[10] P. L. Similon and A. N. Kaufman, Phys. Rev. Lett. **53**, 1061 (1984).
[11] D. A. D'Ippolito and J. R. Myra, Phys. Fluids **29**, 2594 (1986).
[12] S. Meassick, T. Intrator, N. Hershkowitz, J. J. Browning, and R. Majeski, Phys. Fluids B **1**, 1049 (1989).
[13] G. Schimidt, *Physics of High Temperature Plasmas* (Academic Press, New York, 1979), p. 292.
[14] M. Kwon *et al.*, Fusion Sci. Technol. **43(1T)**, 23 (2003).
[15] B. H. Park, N. S. Yoon, S. S. Kim, J. Y. Kim, and M. Kwon, Fusion Sci. Technol. **43(1T)**, 92 (2003).
[16] R. Minami *et al.*, Plasma Phys. Controlled Fusion **44**, 1363 (2002).
[17] S. S. Kim and H. Jhang, Phys. Plasmas **11**, 4088 (2004).